Wettability Effects on Heat Transfer

Chiwoong Choi[1] and Moohwan Kim[2]
[1]University of Wyoming,
[2]Pohang University of Science and Technology
[1]United States
[2]Republic of Korea

1. Introduction

Wettability is an ability of a liquid to maintain contact with a solid surface. Most of heat transfer systems are considered that of an intermediate fluid on a solid surface. Thus, the wettability has a potential of being effective parameter in the heat transfer, especially a two-phase heat transfer. In the two-phase states, there are triple contact lines (TCL), which are the inter-connected lines for all three phases; liquid, gas, and solid. All TCL can be expanded, shrunken, and moved during phase change heat transfer with or without an external forced convection. This dynamic motion of the TCL should be balanced with a dynamic contact, which is governed by the wettability. Recently, interesting phenomena related with superhydrophilic/ hydrophobic have been reported. For example, an enhancement of both the heat transfer and the critical heat flux using the hydrophobic and hydrophilic mixed surface was reported by Betz et al. (2010). Various heat transfer applications related with these special surfaces are accelerated by new micro/nano structured surface fabrication techniques, because the surface wettability can be changed by only different material deposition (Phan et al., 2009b). In addition, many heat transfer systems become smaller, governing forces change from a body force to a surface force. This means that an interfacial force is predominant. Thus, the wettability becomes also one of influential parameters in the heat transfer.

This chapter will be covered by following sub parts. At first, a definition of the wettability will be explained to help an understanding of the wettability effects on various heat transfer mechanisms. Then, previous researches for single phase and two-phase heat transfer will be reviewed. In the single phase, there is no TCL. However, there is an apparent slip flow on a hydrophobic surface. Most studies related to a slip flow focused on the reduction of a frictional pressure loss. However, several studies for wettability effects in a convective heat transfer on a hydrophobic surface were carried out. So, this part will be covered by the slip flow phenomenon and the convective heat transfer related to the slip flow on the hydrophobic surface. In the two-phase flow, various two-phase heat transfers including evaporation, condensation, pool boiling, and flow boiling will be discussed. In evaporation and condensation parts, previous studies related with the wettability effects on the evaporation and the condensation of droplets will be focused on. Most studies for the wettability effects are included in the pool boiling heat transfer field. In the pool boiling heat transfer, bubbles are incepted and departed with removing heat from the heated surface. After meeting a maximum heat flux, which is limited by higher resistance of vapor phase columns on the heating surface, boiling heat transfer is deteriorated before meeting a

melting temperature of material of the heating surface. Therefore, how many bubbles are generated on the surface and how frequently bubbles are departed from the surface are important parameters in the nucleate boiling heat transfer. Obviously, there are two-phase interfaces on the heated solid surface like as situations of incepted bubble, moving bubble, and vapor columns. Therefore, these all sequential mechanisms are affected by the wettability. In this part, the wettability effects on bubble inception, nucleate boiling heat transfer, and CHF will be reviewed. Lastly, previous works related with wettability effects on flow boiling in a microchannel will be reviewed.

2. What is wettability?

2.1 Fundamentals of wetting phenomena

The wettability represents an ability of liquid wetting on a solid surface. Surface force (adhesive and cohesive forces) controls the wettability on the surface. The adhesive forces between a liquid and a solid cause a liquid drop to spread across the surface. The cohesive forces within the liquid cause the drop to avoid contact with the surface. A sessile drop on a solid surface is typical phenomena to explain the wettability (Fig. 1).
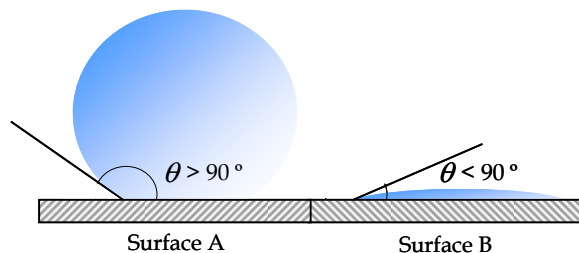

Fig. 1. Water droplets on different wetting surfaces

The surface A shows a fluid with less wetting, while the surface B shows a fluid with more wetting. The surface A has a large contact angle, and the surface B has a small contact angle. The contact angle (θ), as seen in Fig. 1, is the angle at which the liquid-vapor interface meets the solid-liquid interface. The contact angle is determined by the resultant between adhesive and cohesive forces. As the tendency of a drop to spread out over a flat, solid surface increases, the contact angle decreases. Thus, a good wetting surface shows lower a contact angle and a bad wetting surface shows a higher contact angle (Sharfrin et al., 1960). A contact angle less than 90° (low contact angle) usually indicates that wetting of the surface is very favorable, and the fluid will spread over a large area of the surface. Contact angles greater than 90° (high contact angle) usually indicates that wetting of the surface is unfavorable, so the fluid will minimize contact with the surface. For water, a non-wettable surface hydrophobic (Surface A in Fig.1) and a wettable surface may also be termed hydrophilic (Surface B in Fig.1). Super-hydrophobic surfaces have contact angles greater than 150°, showing almost no contact between the liquid drop and the surface. This is sometimes referred to as the Lotus effect. The table 1 describes varying contact angles and their corresponding solid/liquid and liquid/liquid interactions (Eustathopoulos et al., 1999). For non-water liquids, the term lyophilic and lyophobic are used for lower and higher contact angle conditions, respectively. Similarly, the terms omniphobic and omniphilic are used for polar and apolar liquids, respectively.

There are two main types of solid surfaces with which liquids can interact: high and low energy type solids. The relative energy of a solid has to do with the bulk nature of the solid itself. Solids such as metals, glasses, and ceramics are known as 'hard solids' because the chemical bonds that hold them together (e.g. covalent, ionic, or metallic) are very strong. Thus, it takes a large input of energy to break these solids so they are termed high energy. Most molecular liquids achieve complete wetting with high-energy surfaces. The other type of solids is weak molecular crystals (e.g. fluorocarbons, hydrocarbons, etc.) where the molecules are held together essentially by physical forces (e.g. van der waals and hydrogen bonds). Since these solids are held together by weak forces it would take a very low input of energy to break them, and thus, they are termed low energy. Depending on the type of a liquid chosen, low-energy surfaces can permit either complete or partial wetting. (Schrader & Loeb, 1992; Gennes et al., 1985).

Contact angle	Degree of wetting	Strength	
		Solid/Liquid	Liquid/Liquid
$\theta = 0°$	Perfect wetting	strong	weak
$0 < \theta < 90°$	high wettability	strong	strong
$90° \leq \theta < 180°$	low wettability	weak	weak
$\theta = 180°$	Perfectly non-wetting	weak	strong

Table 1. Contact angle and wettability

2.2 Wetting models

There are several models for interface force equilibrium. An ideal solid surface is one that is flat, rigid, perfectly smooth, and chemically homogeneous. In addition, it has zero contact angle hysteresis. Zero hysteresis implies that the advancing and receding contact angles are equal. In other words, there is only one thermodynamically stable contact angle. When a drop of liquid is placed on such a surface, the characteristic contact angle is formed as depicted in Fig. 1. Furthermore, on an ideal surface, the drop will return to its original shape if it is disturbed (John, 1993).

Laplace's theorem is the most general relation for the wetting phenomena. It indicates a relation of pressure difference between inside and outside of an interface as like Eq. (1) (Adamson, 1990),

$$\Delta p = \gamma \left(\frac{1}{R_1 + R_2} \right) = \gamma \kappa \tag{1}$$

where, γ is a surface tension coefficient, R_1 and R_2 are radius of the interface, κ is a curvature of the interface. In equilibrium, the net force per unit length acting along the boundary line among the three phases must be zero. The components of net force in the direction along each of the interfaces are given by Young's equation (Young, 1805),

$$\gamma_{SG} = \gamma_{SL} + \gamma_{LG} \cos \theta \tag{2}$$

which relates the surface tensions among the three phases: solid, liquid and gas. Subsequently this predicts the contact angle of a liquid droplet on a solid surface from knowledge of the three surface energies involved. This equation also applies if the gas phase is another liquid, immiscible with the droplet of the first liquid phase.
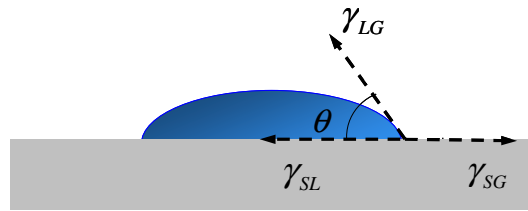
Fig. 2. Contact angle of a liquid droplet wetted to a solid surface

Unlike ideal surfaces, real surfaces do not have perfect smoothness, rigidity, or chemical homogeneity. Such deviations from ideality result in phenomena called contact-angle hysteresis. The contact-angle hysteresis is defined as the difference between the advancing (θ_a) and receding (θ_b) contact angles (Good, 1992):

$$H = \theta_a - \theta_r \tag{3}$$

In simpler terms, contact angle hysteresis is essentially the displacement of a triple contact line (TCL), by either expansion or retraction of the droplet.
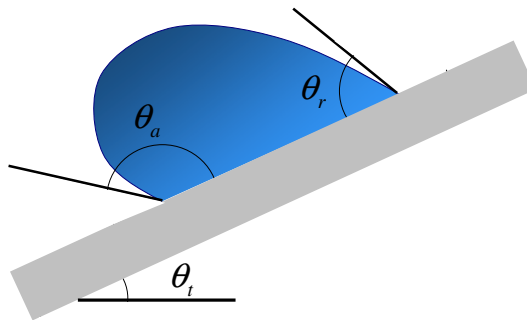

Fig. 3. Schematics of advancing and receding contact angles

Fig. 3 depicts the advancing and receding contact angles. Here, θ_t is an inclined angle. The advancing contact angle is the maximum stable angle, whereas the receding contact angle is the minimum stable angle. The contact-angle hysteresis occurs because there are many different thermodynamically stable contact angles on a non-ideal solid. These varying thermodynamically stable contact angles are known as metastable states (John, 1993). Such motions of a phase boundary, involving advancing and receding contact angles, are known as dynamic wetting. When a contact line advances, covering more of the surface with liquid, the contact angle is increased, it is generally related to the velocity of the TCL (Gennes, 1997). If the velocity of a TCL is increased without bound, the contact angle increases, and as it approaches 180° the gas phase it will become entrained in a thin layer between the liquid and solid. This is a kinetic non-equilibrium effect, which results from the TCL moving at such a high speed, that complete wetting cannot occur.

A well-known departure from an ideality is when the surface of interest has a rough texture. The rough texture of a surface can fall into one of two categories: homogeneous or heterogeneous. A homogeneous wetting regime is where the liquid fills in the roughness

grooves of a surface. On the other hand, a heterogeneous wetting regime is where the surface is a composite of two types of patches. An important example of such a composite surface is one composed of patches of both air and solid. Such surfaces have varied effects on the contact angles of wetting liquids. Wenzel and Cassie-Baxter are the two main models that attempt to describe the wetting of textured surfaces. However, these equations only apply when the drop size is sufficiently large compared with the surface roughness scale (Marmur, 2003).

The Wenzel model describes the homogeneous wetting regime, as seen in Fig. 4(a), and is defined by the following equation for the contact angle on a rough surface (Wenzel, 1936):

$$\cos\theta^* = \beta\cos\theta \tag{4}$$

where, θ^* is the apparent contact angle which corresponds to the stable equilibrium state (i.e. minimum free energy state for the system). The roughness ratio, β, is a measure of how surface roughness affects a homogeneous surface. The roughness ratio is defined as the ratio of a true area of the solid surface to the apparent area. Also, θ is the Young contact angle as defined for an ideal surface in Eq. (2). Although Wenzel's equation demonstrates that the contact angle of a rough surface is different from the intrinsic contact angle, it does not describe contact angle hysteresis (Schrader and Loeb, 1992).

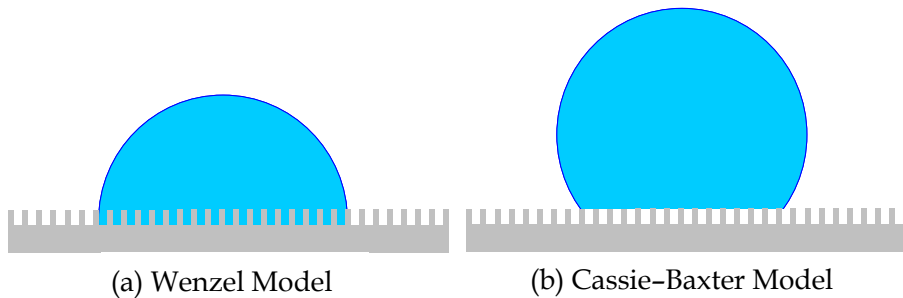(a) Wenzel Model   (b) Cassie–Baxter Model

Fig. 4. Models for rough surface: (a) Wenzel model and (b) Cassie-Baxter model

When dealing with a heterogeneous surface, the Wenzel model is not sufficient. This heterogeneous surface, like that seen in Fig. 4(b), is explained by using the Cassie-Baxter equation (Cassie's law): (Cassie & Baxter, 1944; Marmur, 2003)

$$\cos\theta^* = \beta_f f \cos\theta_Y + f - 1 \tag{5}$$

Here the β_f is the roughness ratio of the wet surface area and f is the fraction of solid surface area wet by the liquid. Cassie-Baxter equation with $f = 1$ and $\beta_f = \beta$ is identical to Wenzel equation. On the other hand, when there are many different fractions of surface roughness, each fraction of the total surface area is denoted by f_i. A summation of all f_i equals 1 or the total surface. Cassie–Baxter can also be recast in the following equation (Whyman et al., 2008):

$$r\cos\theta^* = \sum_{n=1}^{N} f_i \left(\gamma_{i,SG} - \gamma_{i,SL} \right) \tag{6}$$

here, γ is the Cassie-Baxter surface tension between liquid and gas, the $\gamma_{i,SG}$ is the solid gas surface tension of every component and $\gamma_{i,SL}$ is the solid liquid surface tension of every component. A case that is worth mentioning is when the liquid drop is placed on the substrate, and it creates small air pockets underneath it. This case for a two component system is denoted by: (Whyman et al., 2008)

$$\gamma\cos\theta^{*} = f_1\left(\gamma_{1,SG}-\gamma_{1,SL}\right)+\left(1-f_1\right)\gamma \tag{7}$$

Here, the key difference in notice is that the there is no surface tension between the solid and the vapor for the second surface tension component. This is because we assume that the surface of air that is exposed is under the droplet and is the only other substrate in the system. Subsequently, the equation is then expressed as (1 - f). Therefore, the Cassie equation can be easily derived from the Cassie–Baxter equation. Experimental results regarding the surface properties of Wenzel versus Cassie–Baxter systems showed the effect of pinning for a Young angle of 180° to 90°, a region classified under the Cassie–Baxter model. This liquid air composite system is largely hydrophobic. After that point a sharp transition to the Wenzel regime was found where the drop wets the surface but no further than edges of the drop. A third state is the penetration state where the drop is in the Wenzel state but also fills a region of the substrate around the drop. A drop placed on a rough surface can be either in Cassie-Baxter, Wenzel or penetration states. Furthermore, can easily change its state if the required barrier energy is gained by the drop, e.g. if the drop is deposited from some height (He et al., 2003) or by applying pressure (Lafuma & Quere, 2003) on the drop to fill the cavities with liquid. The equilibrium state depends on whether, for given θ, β, ϕ_s, the minimum energy is of Wenzel type or of Cassie-Baxter type. With the critical contact angle,

$$\theta_c = \cos^{-1}\left[\left(\phi_s-1\right)/\left(r-\phi_s\right)\right] \tag{8}$$

such as when θ > θ_c, the most stable state is Cassie-Baxter's one, whereas when θ < θ_c, it is Wenzel's one. A transition from a metastable (e.g., Cassie-Baxter) state to the most stable (e.g., Wenzel) state is possible only if the required energy barrier is overcome by the drop (e.g., by lightly pressing the drop). These characteristics of models will be shown in literatures related with drop-wise evaporation and condensation in hydrophobic surfaces.

3. Wettability effects on heat transfer

3.1 Convective heat transfer

Wettability is highly related with a two-phase interface on a solid surface. So, there is less investigation for a single phase heat transfer. However, the reduction of drag in a hydrophobic tube is one topic related with wettability effects on a single phase flow (Watanabe, 1999). In a hydrophobic surface generally, a no slip condition is not applicable due to the slip flow. Studies of the slip flow on a hydrophobic surface have been conducted both by using an experimental approach (Zhu & Granick, 2002; Barrat & Bocquet, 1999; Tretheway & Meinhart, 2005) and by using a molecular dynamics (MD) approach (Thomson & Troian, 1997; Nagayama & Cheng, 2004). Fluid molecules tumble along the wall much like two solid surfaces sliding over one another occurs when the forces between the fluid and wall molecules are not strong enough to overcome the shear forces at the wall. This

decoupling of the fluid from the wall results in a lower frictional pressure drop. Fig. 5 shows velocity profiles for no slip and slip walls, where u_{slip} is a slip velocity and L_{slip} is a slip length. The velocity for flow between parallel plates with the no slip is given by

$$\frac{u}{u_c} = \left(1 - \left(\frac{y}{w}\right)^2\right) \tag{9}$$

Where u is the fluid velocity, u_c is the maximum velocity, y is the vertical height with centerline of its origin and w is a half of the channel height. In a slip condition, Eq.(9) can be changed to

$$u = u_c \left(1 - \left(\frac{y}{w}\right)^2\right) + u_{slip} \tag{10}$$

Most studies have shown that there is a critical wall shear rate for the onset of the slip. Thomson & Troian (1997) firstly showed the critical shear rate using a MD simulation. Wu & Cheng (2003) reported that the critical shear rate is an order of 50,000 s^{-1} and Zhu & Granick (2002), and Choi et al. (2003) reported that is the order of 10,000 s^{-1}. Usually, slip phenomena have been seen in a microchannel due to a higher shear rate in a smaller dimension. Navier's hypothesis effectively describes the slip velocity at a surface is proportional to the shear rate at the surface (Lamb, 1932).

$$u_{slip} = L_{slip} \left.\frac{du}{dy}\right|_{wall} \tag{11}$$
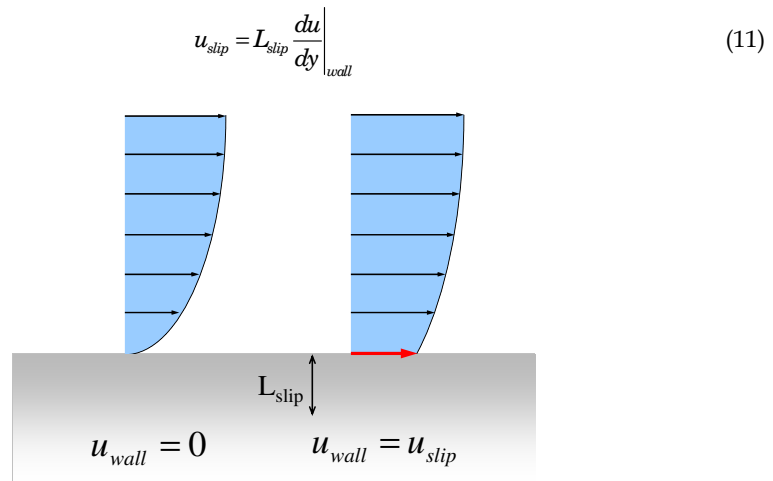

$$u_{wall} = 0 \qquad u_{wall} = u_{slip}$$

Fig. 5. Schematics of no slip and slip velocity profiles

Various researchers also proposed models for the slip length. Tretheway & Meinhart (2005) suggested possible mechanisms of the slip flow on a hydrophobic surface, which is existence of nanobubbles or a layer of lower density fluid at the surface. Also, they proposed the slip length as a function of an air gap and a plate height with rarefied gas conditions.

Now, we will discuss about wettability effects on a convective heat transfer according to slip flow on a hydrophobic surface. Here we will review three reports for this topic. First, Wu & Cheng (2003) studied surface condition effects on laminar convective heat transfer in

microchannels for water. They fabricated 13 different trapezoidal silicon microchannels. Also, three of them were coated with silicon oxide to increase their hydrophilic abilities (Asif et al., 2002). The Nusselt number of microchannels with the hydrophilic silicon oxide surface is higher than that with the hydrophobic silicon surface, which means the hydrophilic capability of the surface enhance the convective heat transfer (Fig. 6). However, they did not explain the physical reason.
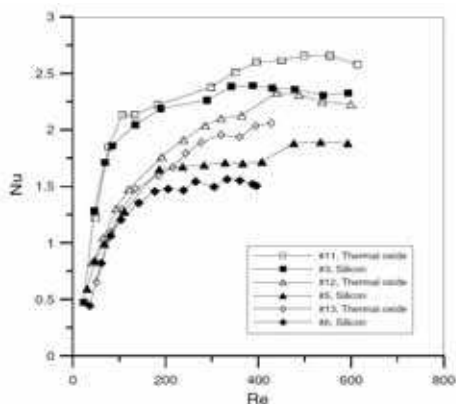

Fig. 6. Effect of surface wettability on Nusselt number: #11(L/D_h~307), #3(L/D_h~310), #12(L/D_h~368), #5(L/D_h~370), #13(L/D_h~451), #6(L/D_h~451) (Wu & Cheng, 2003)

Second, Rogengarten et al. (2006) investigated the effect of contact angle on the convective heat transfer in a microchannel. They analytically derived the Nusselt number using a slip velocity condition, as it follows:

$$Nu_{slip} = \frac{4\left(\frac{4}{3} + 2A\right)}{\left[1.32 - A\left(3.7 + \frac{8}{3}A\right)\right]} \tag{12}$$

where, A = u_{slip}/u_c, a ratio of a slip velocity and a maximum velocity. Fig. 7 shows Nusselt number increased by approximately 2% for a 10% ratio of slip velocity as its maximum velocity.

Fig. 8 indicates that higher contact angle surfaces tend to decrease that heat transfer coefficient comparing with lower contact angle surfaces. Also, this deviation can occurred in over the specific Peclet number (Pe~100), which the slip flow occurred.

Lastly, Hsieh & Lin (2009) performed experiments to study the convective heat transfer in rectangular microchannels using deionized (DI) water, methanol, 50 wt% DI water/50 wt% methanol mixture and ethanol solutions. The hydrophilic and hydrophobic surfaces were obtained using Ultra Violet (UV) treatment. They measured flow and temperature fields using a micro particle image velocimetry (μPIV) and a micro laser-induced fluorescence (μLIF), respectively. In their experiments, maximum slip ratio is 10% for water in the hydrophobic microchannel. Also, their results indicate that the hydrophilic microchannel has higher local heat transfer coefficient than the hydrophobic microchannel (Fig. 9).
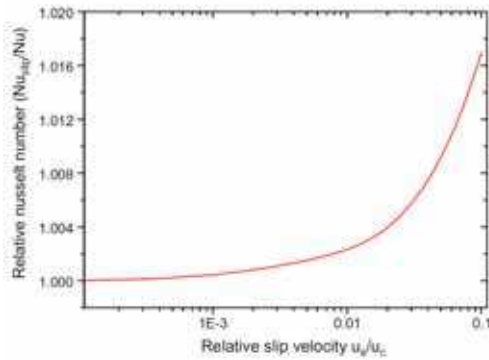
Fig. 7. Relative change in the Nusselt number due to slip induced flow-rate variations (Rogengarten et al., 2006)
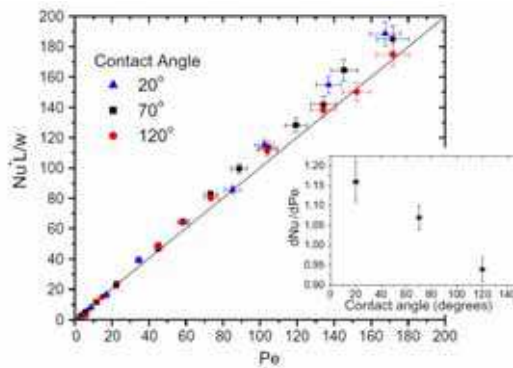

Fig. 8. Ratio of nondimensional heat flux as a function of Pe for a different contact angle. Insert shows the gradient of Nu v.s. Pe graph as a function of contact angel for Pe > 100 (Rogengarten et al., 2006)
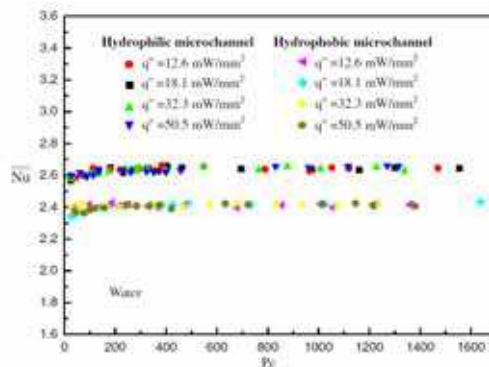

Fig. 9. Nu vs Pe for hydrophilic and hydrophobic microchannels (Hsieh & Lin, 2009)

3.2 Two-phase heat transfer

3.2.1 Evaporation

Evaporation is one of major two-phase heat transfer mechanisms. In an evaporation process, a mass transfer occurs, which means liquid meniscus including a triple contact line (TCL) has a motion. Therefore, we need to consider a dynamic contact angle (advancing and receding contact angles) as shown in Fig. 3. Generally, the advancing contact angle will tend to toward a lower value during evaporation (Picknett & Bexon, 1977). Most of studies for wettability effects on the evaporation fundamentally are focused on an evaporation of a sessile drop. The evaporation process of the droplet can be classified to few steps as shown in Fig.10: Step 1 (saturation of atmosphere), Step 2 (constant contact radius with a decreasing drop height and contact angle), Step 3 (a constant contact angle with a decreasing a contact radius) and Step 4 (final drop disappearance). In most previous studies focused on step 2, 3, and 4.

Chandra et al. (1996) studied on the contact angle effect on the droplet evaporation. Three kinds of droplets of pure water, surfactant 100 ppm and 1000 ppm on a stainless steel surface were visualized. Their results indicate that a reduced contact angle makes a droplet thickness thinner and a contact area larger. Thus, an increased heat transfer area and a decreased conductive resistance enhance the droplet evaporation (Fig. 11). Takata et al. (2004, 2005) measured an evaporation time, a wetting limit and Leidenfrost temperatures on stainless steel, copper and aluminum surfaces. They used a plasma-irradiation to increase a wetting property of those surfaces. Their results indicate that the evaporation time decreases and the wetting limit and the Leidenfrost temperatures increase in hydrophilic surfaces. Therefore, the hydrophilic surface has potentials for the enhancement of evaporation.
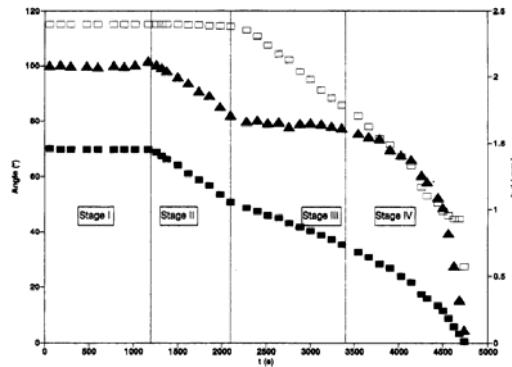

Fig. 10. Evaporation process for water on ETFE with initial drop volume of 5 μL: □ Diameter, ■ Height, and ▲ Angle (Bourges-Monnire & Shanahan, 1995)

Yu et al. (2004) reported an evaporation of water droplets on self-assembled monolayers (SAMs) follows an exclusive trend from a constant contact diameter model to a constant contact angle mode. Shin et al. (2009) investigated droplet evaporations on pure glass, octadecyl-tricholoro-silane (OTS), and alkyl-ketene dimmer (AKD) surfaces. They show that a hydrophilic surface enhances the evaporation heat transfer and a super-hydrophobic surface does not have distinct stages and pinning sections. Kulinich & Farzaneh (2009) investigated a contact angle hysteresis effect on a droplet evaporation using two super-hydrophobic surfaces of the same contact angle but contrasting wetting hysteresis. In their results, the surface of a low contact angle hysteresis was observed to follow the evaporation

model normally ascribed to hydrophobic surface (a quasi-static constant angle while constantly decreasing contact diameter). Meanwhile, the surface with a high contact angle hysteresis was found to be behaved in accordance with the evaporation model normally associated with hydrophilic surfaces (constantly the decreasing contact angle and the quasi-static contact diameter).
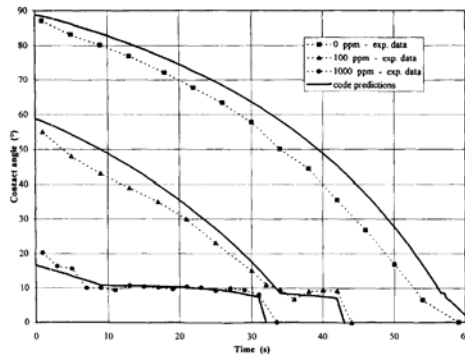

Fig. 11. Evolution of contact angle during evaporation of droplets of pure water, 100 ppm and 1000 ppm surfactant solutions on a stainless steel surface at 80 °C, (Chandra et al., 1996)
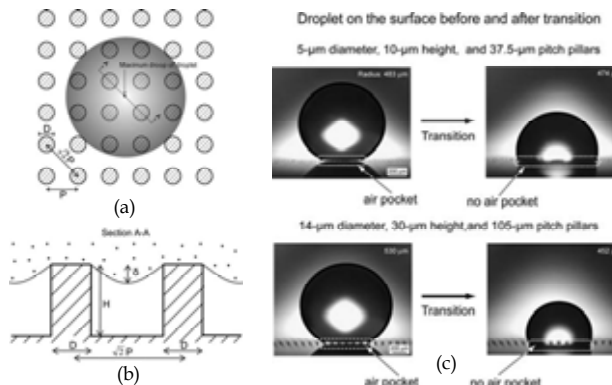

Fig. 12. A small water droplet suspended on a super-hydrophobic surface consisting of a regular array of circular pillars. (a) Plan view. (b) Side view in section A–A, (c) Visualization results for transition (Jung & Bhushan, 2007)

Jung & Bhushan (2007) studied effects of a droplet size on the contact angle by evaporation using droplets with radii ranging from about 300 to 700 µm. In addition, they proposed a criterion where the transition from the Cassie and Baxter regime to the Wenzel regime occurs when the droop of the droplet sinking between two asperities is larger than the depth of the cavity. A small water droplet is suspended on a super-hydrophobic surface consisting of a regular array of circular pillars with diameter D, height H and pitch P as shown in Fig. 12(a). The curvature of a droplet is governed by the Laplace equation, which relates the pressure inside the droplet to its curvature (Adamson, 1990). Therefore, the maximum droop of the droplet (δ) in the recessed region can be found in the middle of two pillars that

are diagonally across as shown in Fig. 12(b) which is if the droop is much greater than the depth of the cavity,

$$\left(\sqrt{2}P - D\right)^2 / R \geq H \qquad (13)$$

Then, the droplet will just contact the bottom of the cavities between pillars, resulting in the transition from the Cassie and Baxter regime to the Wenzel regime as shown in Fig. 12(c). Before the transition, an air pocket is clearly visible at the bottom area of the droplet, but after the transition air pocket is not found at the bottom area of the droplet.
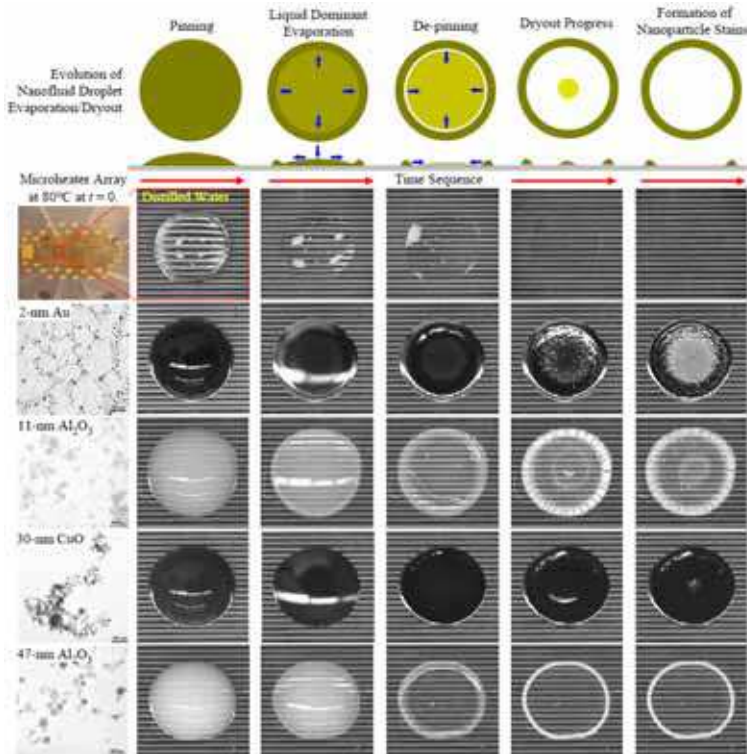

Fig. 13. Evaporation and dryout of various nanofluids on a microheater array, (Chon et al. http://minsfet.utk.edu/Research/2007-update/Evaporation_Dryout.pdf)

Nanofluids have various engineering merits including higher conductivity, enhancement of boiling heat transfer and CHF. Especially, the nano-particle deposited surface shows super-hydrophilic characteristics. Based on this good wetting property, several studies for the evaporation of a nanofluid have been conducted (Leeladhar et al., 2009; Sefiane & Bennacer, 2009; Chen et al., 2010). The initial equilibrium contact angle of the nanofluids was significantly affected by the nanoparticle sizes and concentrations. During evaporation, the evaporation behavior for the nanofluids exhibited a complete different mode from that of the base fluid. In terms of a contact angle, nanofluids shows a slower decrease rate than base fluid. A nanofluid contact diameter remained almost a constant throughout evaporation

with a slight change only at the very end of an evaporation stage. The nanofluids also show a clear distinction in the evaporation rates, resulting in a slower rate than base fluid. No abrupt change in a contact angle and a diameter was observed during the evaporation, the deposited nanoparticles after the complete evaporation of a solvent showed unique dry-out patterns depending on nanoparticle sizes and concentrations, e.g., a thick ring-like pattern (as shown in Fig. 13) with larger particle sizes while a uniformly distributed pattern with smaller particles at higher concentrations.

3.2.2 Condensation

Here, we will show short reviews for wettability effects on a condensation including fundamentals and systematic views. Most studies for wettability effects on condensation are also focused on a droplet condensation mechanism like as evaporation. Fritter et al. (1991) has identified different stages of a droplet growth during condensations of a vapor on partially wetting surfaces. An initial stage where a surface coverage by the condensate is very low and there is negligible coalescence, a second stage where in the droplets grow and coalesce with no new droplets appearing in the empty spaces between the already existing drops. The droplet growth then attains a self similar pattern with time. The surface coverage attains a constant value of 0.5 with appearing no new drops. The growth of drops before coalescence is less when compared to the growth after the drops coalescence. They proposed a growth rate of an individual drop and after drop coalescence is exponent of 1/3 and 1 of time, respectively (Fig. 14).
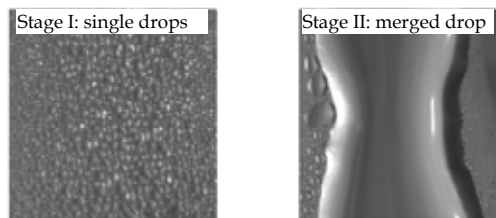

Fig. 14. A condensed drop in the hydrophilic surface: different stages in a condensation (Pulipak, 2003)

It is a well-known experimental fact that, in a drop-wise condensation, most of the heat transfer occurs during the early stages of the formation and the growth of a droplet (Griffith, 1972). Therefore, it must therefore be the aim of any pretreatment of the condenser surface to cause the condensate droplet to depart as early and as quickly from the condenser surface as possible. The departure of the drop, on the other hand, is resisted by the adhesion of the droplet to the condenser surface; this resistance has been attributed to the contact angle hysteresis (Schwartz et al., 1964). A contact angle is formed between a liquid meniscus and solid surface with which it intersects. As a rule, this angle is different in a situation where the liquid advances from the one where it recedes. The actual difference between advancing and receding contact angle is referred to as a contact angle hysteresis. While a contact angle hysteresis stems from dynamic effects, it is to be noted that it also exists under static conditions: advancing a liquid meniscus and stopping it will lead to the static advancing contact angle; receding the meniscus prior to a static measurement will yield the static receding contact angle. The difference between the two contact angles, which is as a rule finite, may be termed as the static contact angle hysteresis. Gokhale et al. (2003) conducted

measurements of the apparent contact angle and the curvature of a drop and meniscus during condensation and evaporation processes in a constrained vapor bubble (CVB) cell. A working fluid and a surface material are n-butanol and quartz, respectively. They monitored a growth of a single drop until that drop merges with another drop. They found an apparent contact angle is a constant during condensation. As the rate of condensation increases, the contact angle increases. This means that a dynamic contact angel (shown in Fig. 3) should be considered in drop-wise condensation. Two main causes of static contact angle hysteresis are surface heterogeneity and roughness (Neumann, 1974).

Pulipaka (2003) studied the wettability effects on a heterogeneous condensation as his master thesis. Main objectives of this study are wettability effects on a drop-wise condensation and a drop growth rate. He observed the initial growth rate for the hydrophilic surface is higher than that for the hydrophobic surface. However, at the final stage, there is no difference between the hydrophilic and the hydrophobic surfaces as shown in Fig. 15. An initial growth rate for the hydrophilic and the hydrophobic surfaces are exponent of 0.671 and 0.333, respectively. The condensate growth rate is a strong function of a temperature gradient on the hydrophilic surface than the hydrophobic surface (Fig. 16). The time for initiation of a nucleation is decreased as contact angle decreases.
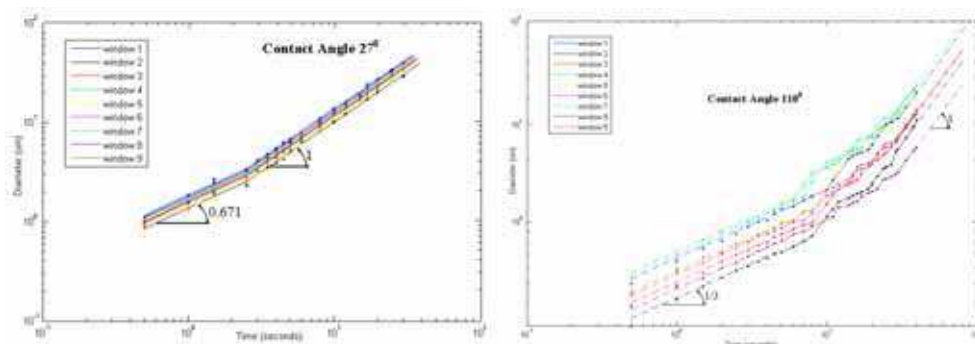

Fig. 15. A diameter of condensed drop for different wettability: left (θ=27 °) and right (θ=110°) (Pulipaka, 2003)
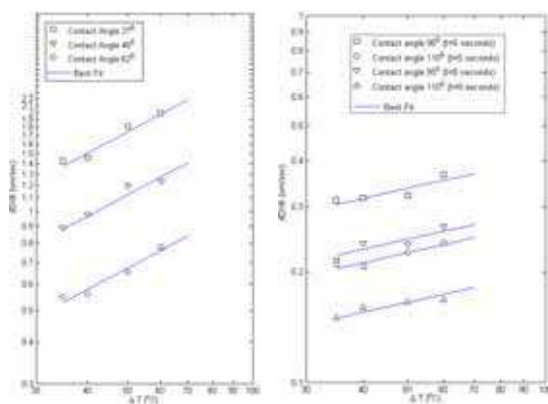

Fig. 16. Drop growth rate with a temperature gradient for different wettabilities (Pulipaka, 2003)

Neumann et al. (1978) studied the effects of varying contact angle hysteresis on the efficiency of a drop-wise condensation heat transfer on a cylinder type condenser. They prepared two kinds of the surface wettability with a coating of Palmitic and Stearic acids. Their results indicate that the heat flux and the heat transfer coefficient increase with the decrease in contact angle hysteresis (increasing the advancing contact angle) (Fig. 17). The limiting size drop to slide on an inclined surface is given in

$$mg\sin\theta_t = \gamma_{LG}\left(\cos\theta_r - \cos\theta_a\right) \tag{14}$$

Therefore, the limiting mass, m for a drop removal will a decrease with decreasing contact angle hysteresis. It enhances the drop-wise condensation heat transfer.
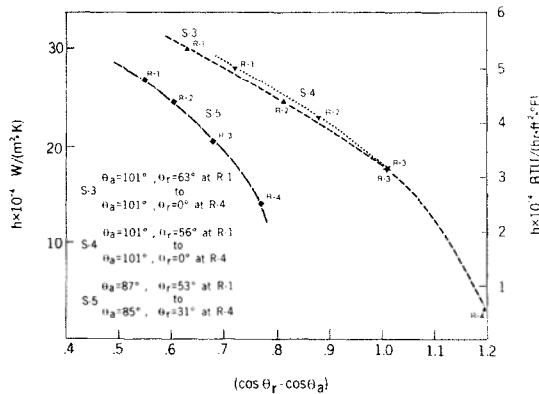

Fig. 17. Heat transfer coefficient, h and contact angle hysteresis (Neumann et al., 1978)

Recently, studies of condensation on the super-hydrophobic surface, which has a micro structured surface have been conducted. Furuta et al. (2010) studied a drop-wise condensation with different hydrophobic surfaces, which are treated with two fluoroalkylsilanes (FAS3 and FAS17). Static contact angles of FAS3 and FAS17 are 146 $^{\circ}$ and 160 $^{\circ}$ for rough surface and 78 $^{\circ}$ and 104 $^{\circ}$, respectively. From this study, the contact angles of the FAS3 or FAS17 coatings decreased concomitantly with a decreasing surface temperature. At the dew point, clear inflection points were observed in the temperature dependence of contact angles as shown in Fig. 18, suggesting the change of the interfacial free energy of the solid-gas interface by water adsorption. The contact angle decrease implies a mode transition from Cassie to Wenzel. The decrease was attributed to the surface wettability change and the increase of the condensation amount of water. The contact angle change attributable to heating revealed that the Wenzel mode is more stable than the Cassie mode.
Narhe & Beysens (2006) studied condensation induced a water drop growth on a super-hydrophobic spike surface. They described three main stages according to the size of the drop (Fig. 19). Initial stage is characterized by the nucleation of the drops at the bottom of the spikes. During intermediate stage, large drops are merged with neighboring small drops. The last stage is characterized by Wenzel-type drops, which growing is similar to that on a planar surface. Also, the contact angle in last stage is smaller than that in the initial stage. When the radius of a drop on the top surface reaches the size of the cavities, two phenomena enter in a competition. The drop can either (i) coalesce with the drops in the

cavity and get sucked in, resulting in a spectacular self-drying of the top surface (Narhe & Beysens, 2004), and/or (ii) coalesce with another drop on the top surface, resulting in a Cassie-Baxter drop (Narhe & Beysens, 2007). If the phenomenon (i) occurs first, condensation results in large Wenzel drops connected to the channels in a penetration regime. If the phenomenon (ii) occurs first, condensation proceeds by Cassie-Baxter drops, thus preserving super-hydrophobicity till stage (i) proceeds and penetration drops are formed. Depending on the pattern morphology, this stage may never occur. Nevertheless, even in the penetration case, some features of super-hydrophobicity are still preserved as the top surface of the micro-structures remained almost dry while the cavities were filled with condensed water. Their results show that Wenzel or Cassie–Baxter states of droplet on the super-hydrophobic structured surface are governed by a length scale of the surface pattern and the structure shape.
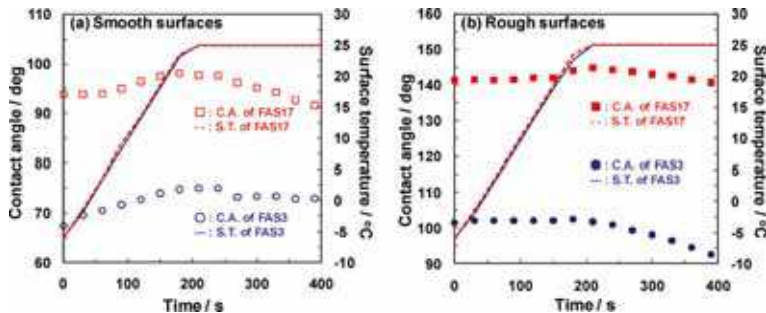

Fig. 18. Contact angle (C.A.) and surface temperature (S.T.) for a different surface wettability and roughness: (a) smooth surfaces, (b) rough surfaces (Furuta et al., 2010)
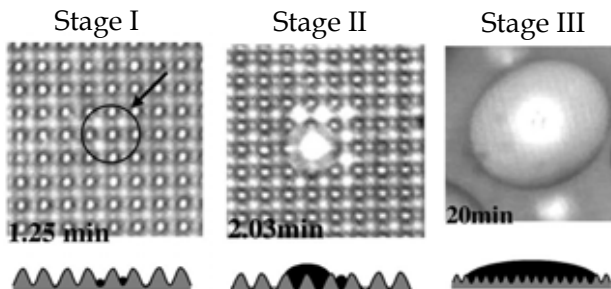

Fig. 19. Three growth stages of condensation (Narhe & Beysens, 2006)

3.2.3 Pool boiling

Many studies of the wettability effects on heat transfer were focused on a pool boiling heat transfer area. A major reason is not related with only the basic two-phase heat transfer mechanism but also the boiling enhancement with nanofluids. In this chapter, we will review previous works for the wettability effects on the pool boiling phenomena including heterogeneous nucleation, nucleate boiling heat transfer and critical heat flux (CHF). Eddington & Kenning (1979) studied the nucleation of gas bubbles from supersaturated solutions of Nitrogen in water and ethanol-water mixtures on two metal surfaces. A

decrease in the contact angle decreases the population of active bubble nucleation sites by reducing the effective radii of individual sites. Wang & Dhir (1993) also reported the same results that the good surface wettability causes a decrease of the density of active nucleation sites. Most of two-phase heat transfer mechanisms are highly related with a contact angle hysteresis due to the dynamics motion of the interface. The contact angle hysteresis is affected by a degree of heterogeneity and roughness of the solid surface (Johnson& Dettre, 1969). Fig. 20 represents the general nucleation and growth processes. Lorenz (1972) developed a theoretical heterogeneous model, which shows the ratio of the bubble radius to the cavity radius, R_1/R_0 is a function of a static contact angle (β_s), a dynamic contact angle (β_d), and a conical cavity half angle (φ). When the static contact angle is fixed and the dynamic contact angle increases, R_1/R_0 increases. Especially, for a highly wetting surface (Fig. 21(a)), the ratio is less than a unity and the effect of dynamic contact angle on R_1/R_0 is significant only when a dynamic contact angle is small. Tong, et al. (1990) proposed a modified Lorenz model, which involved both the static and dynamic contact angles.
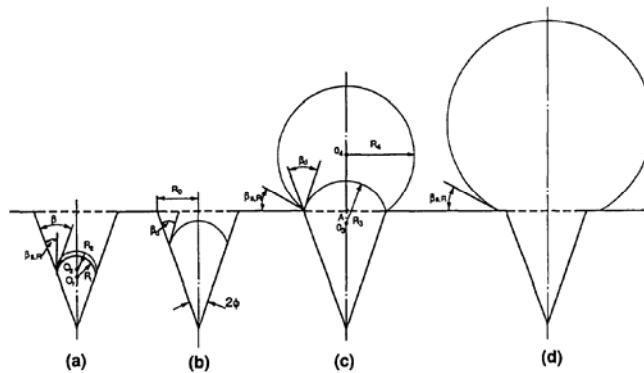

Fig. 20. Bubble growth steps: (a) contact angle readjustment; (b) in-cavity growth; (c) growth on the cavity mouth and the contact angle readjustment; (d) growth on an outer surface (Tong et al, 1990)
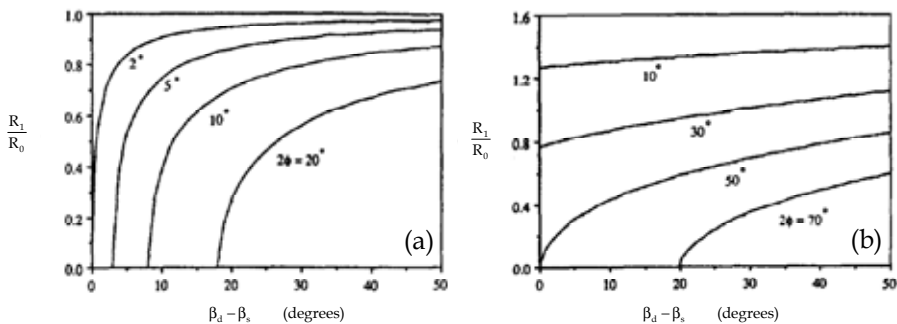

Fig. 21. The effect of the dynamic contact angle on the ratio of embryo radius to the cavity radius for highly wetting liquids: (a) static contact angle = 2°, (b) static contact angle = 50° (Tong et al, 1990)

Yu et al. (1990) conducted experiments of pool boiling using cylindrical heater surfaces of platinum, silicon oxide, and aluminum oxide with dielectric fluids of FC-72 and R-113. They reported the difference in incipience wall superheat value between FC-72 and R-113 was significant, but the surface material effect on a boiling incipience was small.

Harrison & Levine (1958) investigated the wetting effects on the pool boiling heat transfer using different crystal planes of single crystals of copper. In their results, the wetting surface and the non-wetting surface show higher the heat transfer rate in the lower and higher heat flux regions, respectively. The lower heat flux region is governed by a non-boiling natural convection, in which the non-wetting surface represents higher thermal resistance. However, the higher heat flux region is governed by a nucleate boiling, in which the non-wetting surface represents a larger bubble generation due to a higher nucleation cite density (Eddington & Kenning, 1979).

Phan et al. (2009a, 2009b) investigated the wettability effects on a nucleate boiling using various materials deposited on surfaces. In the hydrophobic surface, no bubble departure was noticed and the heat transfer was unstable when the bubbles stayed on the heating surface. In the hydrophilic surface, they measured a departure diameter and a bubble emission frequency. As increased the contact angle, the bubble departure diameter is decreased (Fig. 22a). They compared a following Fritz's correlation (Fritz, 1935), which has linear relation with the contact angle (Eq. 15).

$$D_d = 0.0208\theta \left(\frac{\gamma}{g(\rho_L - \rho_G)} \right)^{0.5} \tag{15}$$

They proposed a new correlation (Eq. 16) for the departure diameter considering the wettability effects using an energy factor, as the ratio of the energy needed to form a bubble with a contact angle to need to form a homogeneous bubble with the same diameter, which is proposed by Bankoff (1967),

$$D_d = 0.626977 \left(\frac{2 + 3\cos\theta - \cos^3\theta}{4} \right) \left(\frac{\gamma}{g(\rho_L - \rho_G)} \right)^{0.5} \tag{16}$$
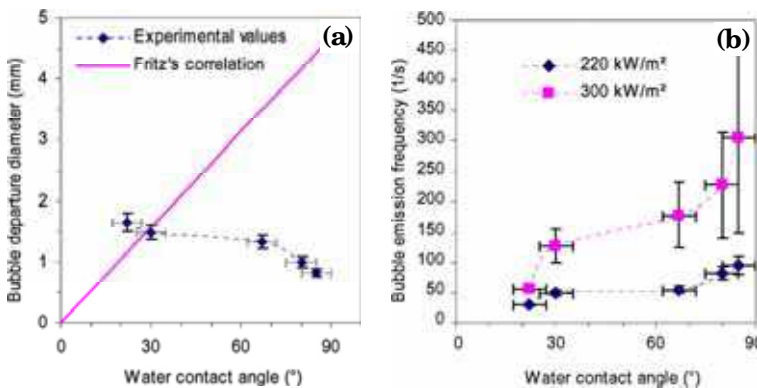

Fig. 22. Wettability effects on a bubble nucleation behavior for the contact angle: (a) Bubble departure diameter and (b) Bubble emission frequency (Phan et al., 2009a)

The decreased contact angle is resulted in the increases of both a bubble growth time (t_g) and a waiting period of the next bubble (t_w) (Fig. 22b). Also, they observed the same trend for density of an active nucleation site with Eddington & Kenning (1979). In their results, a heat transfer coefficient (h) deteriorates with the decrease of the contact angle of between 30 ° and 90 °. When the contact angle is lower than 30 °, its decrease induces an increase of h. Therefore, the highest heat transfer coefficient would be obtained with a surface of which the contact angle of is either 0 ° or 90 °. In contrast, Harada et al. (2010) reported that the bubbles were lifted-off the vertical heated surface of a small contact angle within a shorter period of time after the nucleation than that of a larger contact angle.
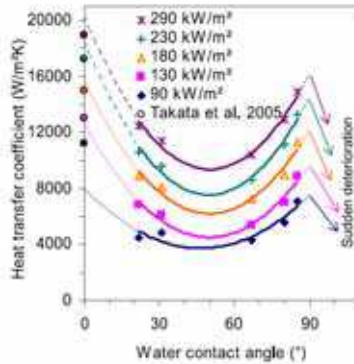

Fig. 23. Heat transfer coefficient versus the contact angles (Phan et al., 2009a)

Except coating methods, a typical way to change the contact angle is the use of surfactant solutions. However, this method changes the surface wettability, the liquid surface tension, and the viscosity simultaneously. It is generally believed that a small amount of surfactant can increase boiling heat transfer. Wasekar & Manglik (1999) reviewed an enhancement of pool boiling using this method. Some studies of wettability effects on the pool boiling with addition of surfactants will be reviewed. Wen & Wang (2010) used water and acetone with different surfactants, 95% sodium dodecyl surfate (SDS), Triton X-100 and octadecylamine. Their result shows that both SDS and Triton X-100 solution can increase the water boiling heat transfer coefficient and the enhancement of heat transfer for SDS solution is obvious. They subtracted only wettability effects on the heat transfer by comparing between SDS and X-100 experiments for the same surface tension and viscosity conditions. The contact angle only for X-100 decreases from 76 to 17 °. It means that the good wettability deteriorates boiling heat transfer.

The most intensively focused topic in the wettability effects in a pool boiling heat transfer is a critical heat flux (CHF), due to its higher dependency of surface characteristics. In the CHF situation, if the surface has ability to supply liquid to evaporate, the CHF can be increased. However, the surface has no ability for that, so the CHF can be decreased, then vapor can cover the entire surface. After reporting the major reason of the CHF enhancement of a nanofluid is wettability (Kim & Kim, 2009). Many researchers have concentrated on the wettability effects on the CHF. Especially, the super-hydrophilic surface that generated during the nanofluid boiling process indicates extremely high CHF value. Gaertner (1965) already reported that a low contact angle results in the higher value of CHF, while a high contact angle results in the lower value of CHF. Kandlikar (2001) proposed a new CHF

model considering the contact angle and the orientation of a heating surface. For a horizontal surface, the correlation becomes Eq. (17),

$$q_{CHF}^{"} = h_{fg}\rho_G^{0.5}\left(\frac{1+\cos\theta}{16}\right)\left[\frac{2}{\pi}+\frac{\pi}{4}(1+\cos\theta)\right]^{0.5}\left[\gamma g\left(\rho_L-\rho_G\right)\right]^{0.25} \tag{17}$$

Various studies for a nanofluid CHF enhancement reported that the major reason of the CHF enhancement is the nanoparticle coated surface, which is changed to a good wetting
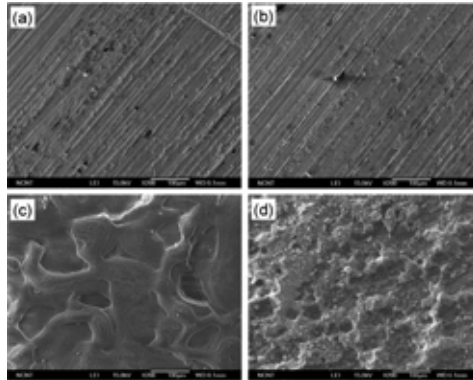

Fig. 24. SEMS images for various copper heater surfaces: (a) fresh, (b) water boiled, (c) alumina-nanofluid boiled, and (d) titania-nanofluid boiled (Kim et al., 2010)
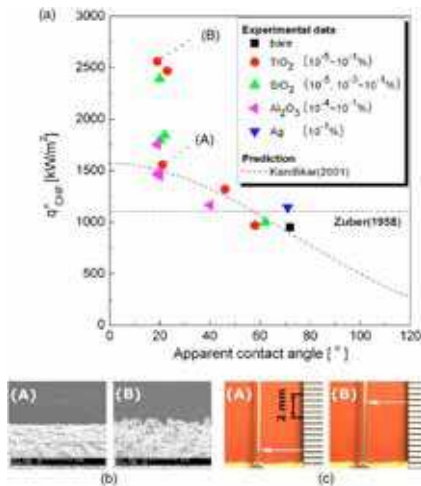

Fig. 25. A relation between CHF and surface characteristics: (a) CHF of pure water vs the contact angle on nanoparticle-deposited surfaces. (b) Scanning electron micrographs and (c) a maximum capillary wicking height of pure water on (A) 10^{-3}% and (B) 10^{-1}% TiO$_2$ nano-particle deposited surfaces with different CHF values at similar contact angles of approximately 20° (Kim & Kim, 2007)

surface. In the other words, the highly wetting surface, which is a lower contact angle, enhances the CHF of the pool boiling (Kim, S. J. et al., 2007; Coursey & Kim, 2008; Kim & Kim; 2009, & Kim, S. et al, 2010). Fig. 24 shows SEM images of the nanoparticle deposited heater surfaces after achieving the CHF. The nanoparticle deposited surface indicates as a highly wetting surface. Kim & Kim (2007) conducted wicking experiments using nano-particle coated wires, which is coated during a nanofluid boiling process. Fig. 25 shows their CHF value corresponding to the contact angle. Their results well agree with the Kandlikar's correlation (Eq. 17), except some cases of the lowest contact angle. These cases of extraordinarily highest CHF show a micro/nano structured surface and a higher wicking height. Chen et al. (2009) observed the same results for a super-hydrophilic surface coated by a nanowire. Kim et al. (2010) conducted a pool boiling CHF experiment using bare silicon, micro-structured (M), nano-structured (N) and both (NM) surfaces. They reported that a NM surface shows the contact angle of 0 $^{\circ}$ (super-hydrophilic) and the highest value of the CHF. Recently, based on the CHF enhancement of the micro/nano structured super-hydrophilic surface, many researchers have been trying to obtain the CHF enhanced surface (Ahn et al., 2010; Truong et al., 2010; Forrest et al., 2010).

3.2.4 Flow boiling

In a conventional system, studies of the wettability effects on a flow boiling are less, because an external flow is dominant comparing with surface force. However, in micro scale, the surface force is predominant because of a higher surface to volume ratio. Choi & Kim (2008) developed a new fabrication technique to study the wettability effects on water flow boiling in a microchannel. They fabricated a single glass rectangular microchannel using a photosensitive glass and six microheaters to measure a local wall temperature and to apply heat to fluid as shown in Fig. 26. A glass was used as a hydrophilic surface and Octadecyl-trichloro-silane (OTS) was coated on a glass surface to obtain a hydrophobic surface. They focused on visualization of the two-phase flow patterns in the microchannel with different wetting surfaces. They observed a new flow pattern in the hydrophobic microchannel, which is named drop-wise slug (Fig. 27). A major flow pattern during a flow boiling in a microchannel is an elongated bubble, which is a very long bubble surrounded with thin liquid film. The evaporation of this thin film is a main heat transfer mechanism in a microchannel (Thome, 2006). Generally, the heat transfer coefficient is initially increased on the lower quality region, gradually decreased at a certain critical quality. A possible reason of this decreasing the heat transfer coefficient is a local dryout (Thome et al., 2004; Dupont et al., 2004). When the local dryout occurred, the liquid film is easily re-wetted on a hydrophilic surface. However, the liquid film is very unstable on a hydrophobic wall (Choi et al, 2010). This unstable pattern is represented to a new flow pattern. His extended work reported the wettability effects on flow boiling in a 500 μm rectangular microchannel for water (Choi et al. (2010). They obtained visualized flow patterns and a local heat transfer coefficient. They observed different flow patterns for different wettability conditions and analyzed heat transfer characteristics based on flow patterns. In the hydrophilic microchannel, flow patterns are similar to previous results for flow boiling in a microchannel. However, in the hydrophobic microchannel, the number of nucleation is increased due to low surface energy as shown in Fig. 28. These results are already reported by the pool boiling studies (Eddington & Kenning, 1979; Wang & Dhir, 1993; Phan et al., 2010a, 2010b). For relatively higher mass flux condition, nucleation is suppressed. They observed a heat transfer trend for different wettabilities and mass fluxes as shown in Fig. 29.
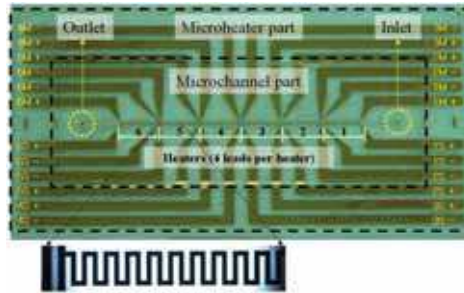
Fig. 26. A single glass microchannel and six gold micro heaters (Choi & Kim, 2008)

Fig. 27. A drop-wise slug flow pattern in a hydrophobic microchannel (Choi & Kim, 2008)

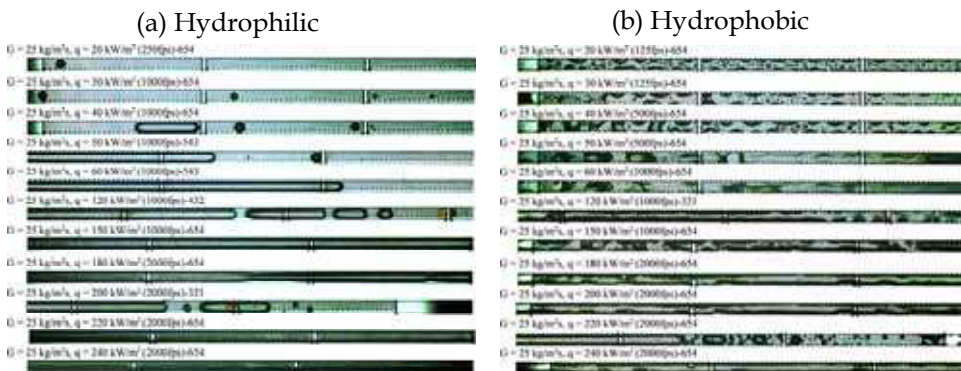(a) Hydrophilic   (b) Hydrophobic

Fig. 28. Two-phase flow patterns in rectangular microchannels for different wettabilities: (a) hydrophilic microchannel, (b) hydrophobic microchannel (Choi et al., 2010)
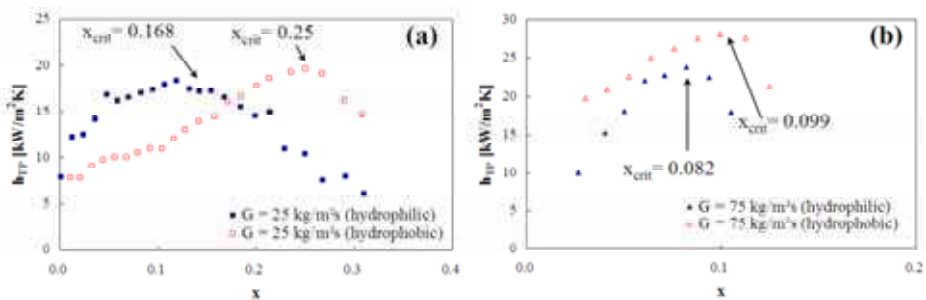

Fig. 29. A local heat transfer coefficient in rectangular microchannels for different wettabilities and mass fluxes: (a) 25 kg/m²s, (b) 75 kg/m²s (Choi et al, 2010)

Zhang et al. (2009) conducted flow boiling experiments with a hydrophobic microchannel with hydrophilic cover glass. They observed wettability effects on two-phase flow patterns as shown in Fig. 30. The tip of the liquid thread (rivulet) penetrates the junction interface of the inlet fluid plenum and the central microchannel at t = 1.0 ms in Fig. 30. Then a churn (chaotic) mushroom cloud, containing a mixture of vapor and liquid, was ejected into the central microchannel. A planar fluid triangle (shrinkage of liquid films), consisting of two contracted liquid films and the mixture of vapor and liquid inside, appears in the central microchannel upstream (see the images for t > 5.0 ms in Fig. 30). In front of the fluid triangle there is a long liquid rivulet populated near the microchannel centerline with the zigzag pattern. The rivulet reached the end of the central microchannel at t = 10.0 ms as shown in Fig. 30(a). For the time t > 12.0 ms, the rivulet was broken in the central microchannel downstream to form isolated droplets (see the circled image at t = 14.0 ms in Fig. 19(a)). The tip of the rivulet is being receded to the central microchannel upstream due to evaporation for t > 12.0 ms in Fig. 30(a), until the whole central microchannel is almost dry out, leaving a short rivulet in the central microchannel upstream (see the images at t=33.0 and 34.0ms in Fig. 30(a)). Then a new rivulet ejection and receding cycle starts. Fig. 30(b) shows the enlarged image for the isolated droplets formed by the breakup of the rivulet. Those new flow patterns are resulted from different wettability and temperature gradient.
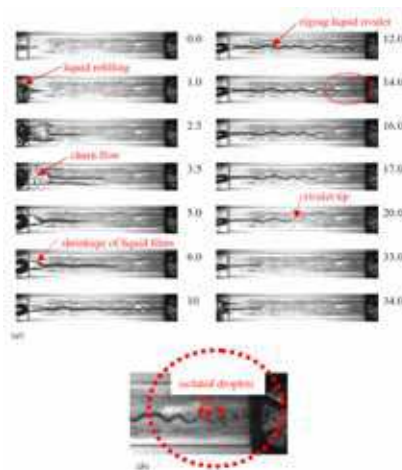

Fig. 30. Periodic liquid rivulet ejection and receding process (Zhang et al., 2009)

There are studies related with the CHF enhancement in the flow boiling in a microchannel. Ahn et al. (2010) conducted experiments with Alumina (Al_2O_3) nanofluid flow boiling on a local small heater to investigate external flow effect. As we discuss previously, nanofluid can enhance CHF in a pool boiling, because a nanofluid makes a super-hydrophilic heating surface during a boiling process. They obtained 40% enhancement of CHF for the highest flow velocity. Also, they measured apparent contact angles for the used heating surfaces. Their results are well agreed with a pool boiling CHF correlation (Eq. 17), except super-hydrophilic surface ($\theta \sim 0^\circ$) as shown in Fig. 31.

Vafaei & Wen (2010) studied CHF of the subcooled flow boiling of Alumina nanofluids in a 510 μm single microchannel. Their results show 51% enhancement of CHF under

nanoparticle concentration of 0.1 vol. %. From their results, a main contribution of CHF enhancement is also a surface modification of nano particles during the boiling process. Sarwar et al. (2007) conducted a flow boiling CHF experiment with a nanoparticle coated porous surface. They reported 25% and 20% enhancement of CHF for Al_2O_3 and TiO_2, respectively. They explained that the enhancement is highly related with a wettability index. In the same group, Jeong et al. (2008) studied the flow boiling CHF with surfactant (TSP) solutions. Their results also show that the surfactant decreases a contact angle of the heating surface, and a CHF enhancement was achieved due to the higher wettability.
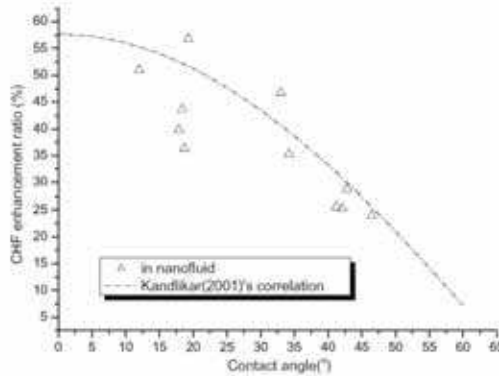

Fig. 31. A relation between the flow boiling CHF enhancement and the contact angle of the heated surface (Ahn et al., 2010)

4. Conclusion

The wettability is an adhesive ability of liquid on a solid surface, which can be characterized with the contact angle. In addition, a solid is used as intermediate to transfer heat thru the working fluid in the most heat transfer problems. Therefore, the wettability has a chance to be one of the important parameters in heat transfer phenomena. Recently, super-hydrophobic/hydrophilic surfaces have shown interesting phenomena, and a major reason of heat transfer enhancement of nanofluids is proven to be a hydrophilic surface coated by oxide nanoparticles. In addition, developed fabrication techniques for the micro/nano structured surface enforce intensive studies for the wettability effects on the heat transfer. In this chapter, we reviewed open literatures related with the wettability effects on the heat transfer. We categorized a single phase and two-phase heat transfers. Moreover, evaporation, condensation, pool boiling, and flow boiling are specifically discussed for the two-phase heat transfer. From these reviews, following consistent conclusions are derived.

The single phase has no TCL, which means that the solid is used as an intermediate to transfer heat thru the working fluid in most heat transfer problems. There is no interface of the two-phase on a solid surface. Therefore, there is less studies related with the wettability effect on the heat transfer. However, there is a slip flow in the hydrophobic surface only when the critical shear rate condition meets. According to previous studies related with the wettability effect on a convective heat transfer shows that the good wetting surface has a higher Nusselt number.

Basically, the wettability is a critical parameter in the two-phase behavior, because the motion of triple contact line (TCL) is highly influenced by a wetting characteristic on the surface. During a phase change heat transfer, mass transfer makes motion of TCL due to a volume expansion or a contraction. Thus, a dynamic wetting including a contact angle hysteresis becomes an influential parameter in the two-phase heat transfer. In evaporation and condensation, we considered the drop-wise heat transfer. In a drop-wise evaporation, the good wetting surface shows a high evaporation rate due to a large heat transfer area and a thin droplet thickness (low heat resistance). In condensation, the wettability effects is dominant on an initial stage of condensation and a good wetting surface shows a higher condensation rate due to the same reason to evaporation. For a super-hydrophilic/hydrophobic surface that was prepared with micro/nano structures, the contact angle hysteresis is the most critical parameter. As well as, morphology is important to understand the heat transfer mechanism in these special surfaces. There are two kinds of modes: Wenzel and Cassie-Baxter, which are governed by the dynamic wetting and the length scale of the surface pattern and the structure shape.

In the pool boiling heat transfer, the wettability is affected on the entire boiling process including a nucleation, a nucleate boiling, and a CHF. The good wettability decreased the density of active nucleation sites and the decreased departure frequency. Therefore, a typical trend for nucleate boiling heat transfer according to wettability effects is that a non-wettable surface indicates higher the heat transfer rate due to a higher nucleation site density. However, there is still unclear understanding for the wettability effects on the nucleate boiling heat transfer, because the nucleate boiling is complicate phenomena mixed surface parameters of a wettability, a roughness, a morphology. In CHF, a good wettability shows the higher value of the CHF due to a liquid supplying ability. For super-hydrophilic surface, there is an additional effect like the morphology for an extraordinary enhancement of the CHF.

In the open literature, there are only few studies related with the wettability effect flow boiling heat transfer owing to fabricational complexities and feasibility in a microscale. Most of studies indicate that the wettability is a critical parameter on the two-phase flow pattern in a microchannel. As same as the CHF in pool boiling, the wettable surface shows a higher value of the CHF in the flow boiling than the non-wettable surface. However, the wettability effects on the heat transfer of the flow boiling are still far from well understanding.

5. References

Adamson, A.V. (1990). *Physical Chemistry of Surfaces*.Wiley, New York, U.S.

Ahn, H. S., Kim, H., Jo, H., Kang, S., Chang, W., & Kim, M. H. (2010). Experimental study of critical heat flux enhancement during forced convective flow boiling of nanofluid on a short heated surface. *Int. J Multiphase Flow*, Vol. 36, pp. 375-384.

Ahn, H. S., Lee, C., Kim, H., Jo, H., Kang, S., Kim, W., Shin, J., & Kim, M. H. (2010). Pool boiling CHF enhancement by micro/nanoscale modification of Zircaloy-4 surface. *Nuclear Engineering and Design*, Vol. 240, pp. 3350-3360.

Asif, S. A. S., Wahl, K. J. & Colton, R. J. (2002). The influence of oxide and adsorbates on the nanomechanical response of silicon surface. *J Mater. Res.*, Vol. 15, No. 2, pp. 546-553.

Bankoff, S. G. (1967). Ebullition from solid surfaces in the absence of a pre-existing gaseous phase. *Trans. Am. Mech. Eng.*, Vol. 79, pp. 735-740.

Barrat, J. & Bocquet, L. (1999). Large slip effect at a nonwetting fluid-solid interface. *Phys. Rev. Lett.*, Vol. 82, No. 3, pp. 4671-4674.

Betz, A. R., Xu, J., Qiu, H., & Attinger, D. (2010). Do surface with mixed hydrophilic and hydrophobic area enhance pool boiling? *Appl. Phys. Lett.*, Vol. 97, pp. 141909-1-141909-3.

Bourges-Monnier, C. & Shanahan, M. E. R. (1995). Influence of Evaporation on Contact Angle. *Langmuir*, Vol. 11, pp. 2820-2829.

Cassie, A. B. D.; Baxter, S. (1944). Wettability of porous surfaces. *Trans. Faraday Soc.*, Vol. 40, pp. 546-551.

Chandra, S., di-Marzo, M., Qiao, Y. M. & Tartarini, P. (1996). Effect of Liquid-Solid Contact Angle on Droplet Evaporation. *Fire Safety Journal*, Vol. 27, pp. 141-158.

Chen, R., Lu, M., Srinivasan, V., Wang, Z., Cho, H. & Majumdar, A. (2009). Nanowires for Enhanced Boiling Heat Transfer. *Nano Letters*, Vol. 9, No. 2, pp. 548-553.

Chen, R., Phuoc, T. X., Martello, D. (2010). Effects of nanoparticles on nanofluid droplet evaporation. *Int. J of Heat Mass Transfer*, Vol. 53, pp. 3677–3682.

Choi, C., Westin, K. J. A. & Breuer, K. S. (2003). Apparent slip flows in hydrophilic and hydrophobic microchannels. *Physics of Fluids*, Vol. 15, No. 10, pp. 2897-2902.

Choi, C. & Kim, M. H. (2008). The fabrication of a single glass microchannel to study the hydrophobicity effect on two-phase flow boiling of water. *J Micromech. Microeng.* Vol. 18, pp. 105016 (9pp).

Choi, C., Shin, J. S., Yu, D. I. & Kim, M. H. (2010). Flow boiling behaviors in hydrophilic and hydrophobic microchannels. *Exp. Therm. and Fl. Sci.*, Vol. 35, pp. 816-824.

Chon, C. H., Paik, S. W., Tipton Jr., J. B. & Kihm, K. D. Evaporation and Dryout of Nanofluid Droplets on a Microheater Array, In: May,1th, 2011, Available from: <http://minsfet.utk.edu/Research/2007-update/Evaporation_Dryout.pdf>

Colin, S., Lalonde, P. & Caen, R. (2004). Validatin of a second-order slip flow model in rectangular microchannels. *Heat Transfer Eng.*, Vol. 25, No. 3, pp. 23-30.

Coursey, J. S., & Kim, J. (2008). Nanofluid boiling: The effect of surface wettability. *Int. J Heat Fluid Flow*, Vol. 29, pp. 1577-1586.

Dupont, V., Thome, J. R. & Jacobi, A. M. (2004). Heat transfer model for evaporation in microchannels. Part II: Comparison with the database. *Int. J Heat Mass Transfer*, Vol. 47, pp. 3387–3401.

Eddington, R. I. & Kenning, D. B. R. (1979). The Effect of Contact Angle on Bubble Nucleation. *Int. J Heat Mass Transfer*, Vol. 22, pp. 1231-1236.

Eustathopoulos, N., Nicholas, M.G. & Drevet, B. (1999). *Wettability at high temperatures*, Oxford, 0080421466, Pergamon, U.K.

Forrest, E., Williamson, E., Buongiorno, J., Hu, L., Rubner, M. & Cohen, R. (2010). Augmentation of nucleate boiling heat transfer and critical heat flux using nanoparticle thin-film coatings. *Int. J Heat Mass Transfer*, Vol. 53, pp. 58-67.

Fritter, D., Knobler, C. M. & Beysens, D. (1991). Experiments and Simulation of Growth of Drops on a Surface. *Physical Review A*, Vol. 43, No. 6, pp. 2858-2869.

Fritz, W. (1935). Maximum volume of vapour bubble. *Phys. Z.*, Vol. 36, pp. 379-384.

Furuta, T., Sakai, M., Isobe, T. & Nakajima, A. (2010). Effect of Dew Condensation on the Wettability of Rough Hydrophobic Surfaces Coated with Two Different Silanes. *Langmuir*, Vol. 26, No. 16, pp. 13305-13309.

Gaertner, R. F. (1965). Photographic Study of Nucleate Pool Boiling on Horizontal Surface. *ASME J Heat Transfer*, Vol. 87, pp. 17-29.

Gennes, P. D. (1997). *Soft Interfaces*. Cambridge University Press, 9780521564175, U.K.

Gennes, P. D. (1985). Wetting: statics and dynamics. *Reviews of Modern Physics*, Vol. 57, No. 3, pp. 827–863.

Gokhale, S. J., Plawsky, J. L. & Wayner Jr., P. C. (2003). Experimental investigation of contact angle, curvature, and contact line motion in dropwise condensation and evaporation. *J Colloid and Interface Science*, Vol. 259, pp. 354-366.

Good, R. J. (1992). Contact angle, wetting, and adhesion: a critical review. *J Adhesion Sci. Technol.*, Vol. 6, No. 12, pp. 1269–1302.

Griffith, P. (1972). *Handbook of Heat Transfer*, McGraw-Hill, New York, U. S.

Harada, T., Nagakura, H., & Okawa, T. (2010). Dependence of bubble behavior in subcooled boiling on surface wettability. *Nuclear Engineering and Design*, Vol. 240, pp. 3949-3955.

Harrison, W. B. & Levine, Z. (1958). Wetting effects on boiling heat transfer: the Copper-Stearic Acid System. *AIChE J*, Vol. 4, No. 4, pp. 409-412.

He, B., Patankar, N. & Lee, J. (2003). Multiple Equilibrium Droplet Shapes and Design Criterion for Rough Hydrophobic Surfaces. *Langmuir*, Vol. 19, pp. 4999-5003.

Hsieh, S. & Lin, C. (2009). Convective heat transfer in liquid microchannels with hydrophobic and hydrophilic surfaces. *Int. J Heat Mass Transfer*, Vol. 52, pp. 260-270.

Jeong, Y. H., Sarwar, M. S. & Chang, S. H. (2008). Flow boiling CHF enhancement with surfactant solutions under atmospheric pressure. *Int. J Heat Mass Transfer*, Vol. 51, pp. 1913-1919.

John, C. B. (1993). *Wettability*, Marcel Dekker, 0824790464, New York, U.S.

Johnson Jr., R. E. and Dettre, R. H. (1969). Wettability and contact angle. *Surface and Colloid Science*, Vol. 2, pp. 85-153.

Jung, Y. C. & Bhushan, B. (2008). Wetting behaviour during evaporation and condensation of water microdroplets on superhydrophobic patterned surfaces. *Journal of Microscopy*, Vol. 229, pp. 127–140.

Kandlikar, S. G. (2001). A theoretical model to predict pool boiling CHF incorporating effects of contact angle and orientation. *AMSE J Heat Transfer*, Vol. 123, pp. 1071-1080.

Kim, S. J., Bang, I. C., Buongiorno, J., & Hu, L. W. (2007). Surface Wettability change during pool boiling of nanofluids and its effect on critical heat flux. *Int. J Heat Mass Transfer*, Vol. 50, pp. 4105-4116.

Kim, H. D. & Kim, M. H. (2007). Effect of nanoparticle deposition on capillary wicking that influences the critical heat flux in nanofluids. *Applied Physics Letters*, Vol. 91, pp. 014104-1-014104-3.

Kim, H., & Kim, M. (2009) Experimental Study of the characteristics and mechanism of pool boiling CHF enhancement using nanofluids. *Heat Mass Transfer*, Vol. 45, pp. 991-998.

Kim, H., Ahn, H. S., & Kim, M. H. (2010). On the Mechanism of Pool Boiling Critical Heat Flux Enhancement in Nanofluids. ASME J. Heat Transfer, Vol. 132, pp. 061501-1-061501-11.

Kim, S. Kim, H. D., Kim, H., Ahn, H. S., Jo, H., Kim, W., & Kim, M. H. (2010). Effects of nano-fluid and surfaces with nano structure on the increase of CHF, *Exp. Therm. Fl. Sci.*, Vol. 4, pp. 487-495.

Kulinich, S. A. & Farzaneh, M. (2009). Effect of contact angle hysteresis on water droplet evaporation from super-hydrophobic surfaces. *Applied Surface Science*, Vol. 255, pp. 4056-4060.

Lafuma, A. & Quere, D. (2003). Superhydrophobic states. *Nature Mater.*, Vol. 2, pp. 457-460.

Lamb, H. (1932). *Hydrodynamics*, Dover, New York, U.S.

Leeladhar, R., Xu, W., & Choi, C. (2009). Effects of Nanofluids on Droplet Evaporation and Wetting on Nanoporous Superhydrophobic Surfaces, *ASME Second International Conference on Micro/Nanoscale Heat and Mass Transfer*, Vol. 2, No. MNHMT2009-18551 pp. 725-733, Shanghai, China, December, 2009.

Lorenz, J. J. (1972). *The effects of surface conditions of boiling characteristics*, Ph. D Thesis, Massachusetts Institute of Technology, Cambridge, Massachusetts.

Marmur, A. (2003). Wetting of Hydrophobic Rough Surfaces: To be heterogeneous or not to be. *Langmuir*, Vol. 19, pp. 8343–8348.

Nagayama, G. & Cheng, P. (2004). Effects of interface wettability on microscale flow by molecular dynamics simulation. *Int. J Heat Mass Transfer*, Vol. 47, pp. 501-513.

Narhe, R. D. & Beysens, D. A. (2004). Nucleation and Growth on a Super-hydrophobic Grooved Surface. *Phys. Rev. Lett.*, Vol. 93, 76103-76107.

Narhe, R. D. & Beysens, D. A. (2006). Water condensation on a super-hydrophobic spike surface. *Europhys. Lett.*, Vol. 75, No. 1, pp. 98–104.

Narhe, R. D. & Beysens, D. A., (2007). Growth Dynamics of Water Drops on a Square-Pattern Rough Hydrophobic Surface. *Langmuir*, Vol. 23, pp. 6486-6489.

Neumann, A. W. (1974). Contact angles and their temperature dependence: thermodynamic status: measurement, interpretation and application. *Adv. Colloid Interface Sci.*, Vol. 4, pp. 105-191.

Neumann, A. W., Abdelmessih, A. H. & Hameed, A. (1978). The role of contact angle and contact angle hysteresis in dropwise condensation heat transfer. *Int. J Heat Mass Transfer*, Vol. 21, pp. 947-953.

Phan, H. T., Caney, N., Marty, P., Colasson, S., & Gavillet, J. (2009a). How does surface wettability influence nucleate boiling? *C.R. Mecanique*, Vol. 337, pp. 251-259.

Phan, H. T, Cabeny, N., Marty, P., Colasson, S., & Gavillet, J. (2009b). Surface wettability control by nanocoating: The effects on pool boiling heat transfer and nucleation mechanism. *Int. J Heat Mass Transfer*, Vol. 52, pp. 5459-5471.

Picknett, R. G. & Bexon, R. (1977). The Evaporation of Sessile or Pendant Drops in Still Air. *J Colloid Interface Sci.*, Vol. 61, No. 2, pp. 336-350.

Pulipaka, S. (2008), *The Effect of Surface Wettability on Heterogeneous Condensation*, Master Thesis, University of Cincinnati, Dept. Mechanical Eng.

Sarwar, M. S., Jeong, Y. H. & Chang, S. H. (2007). Subcooled flow boiling CHF enhancement with porous sruface coatings. *Int. J Heat Mass Transfer*, Vol. 50, pp. 3649-3657.

Sefiane, K., & Bennacer, R. (2009). Nanofluids droplets evaporation kinetics and wetting dynamics on rough heated substrates. *Advances in Colloid and Interface Science*, Vol. 147–148, pp. 263–271.

Schrader, M. E. & Loeb, G.I. (1992). *Modern Approaches to Wettability: Theory and Applications*, Plenum Press, 0306439859, New York, U.S.

Sharfrin, E., Zisman & William, A. (1960). Constitutive relations in the wetting of low energy surfaces and the theory of the retraction method of preparing monolayers. *The Journal of Physical Chemistry*, Vol. 64, No.5, pp. 519–524.

Schwartz, A. M., Rader, C. A. & Huey, E. (1964). Contact angle wettability and adhesion: resistance to flow in capillary systems of positive contact angles. *Adv. Chem. Ser.*, Vol. 43, pp. 250-267.

Shin, D. H., Lee, S. H., Jung, J. & Yoo, J. Y., (2009). Evaporating characteristics of sessile droplet on hydrophobic and hydrophilic surfaces. *Microelectronic Engineering*, Vol. 86, pp. 1350-1353.

Takata, Y., Hidaka, S., Yamashita, A., & Yamamoto, H. (2004). Evaporation of water drop on a plasma-irradiated hydrophilic surface. *Int. J Heat Fluid Flow*, Vol. 25, pp. 320–328.

Takata, Y., Hidaka, S., Cao, J. M., Nakamura, T., Yamamoto, H., Masuda, M., & Ito, T. (2005). Effect of surface wettability on boiling and evaporation. *Energy*, Vol. 30, pp. 209–220.

Thome, J. R. (2006). State-of-the-Art Overview of Boiling and Two-Phase Flows in Microchannels. *Heat Transfer Engineering*, Vol. 27, No. 9, pp. 4-19.

Thome, J. R., Dupont, V. & Jacobi, A. M. (2004). Heat transfer model for evaporation in microchannels. Part I: Presentation of the model. *Int. J Heat Mass Transfer*, Vol. 47, pp. 3375–3385.

Thomson, P. & Troian, S. (1997). A general boundary condition for liquid flow at solid surfaces. *Nature*, Vol. 389, pp. 360-362.

Tong, W., Bar-Cohen, A., Simon T. W. & You, S. M. (1990). Contact angle effect on boiling incipience of highly-wetting liquids. *Int. J Heat Mass Transfer*, Vol. 33, No. 1, pp. 91-103.

Tretheway, D. C. & Meinhart, C. D. (2005). A generating mechanism for apparent fluid slip in hydrophobic microchannel. *Physics of Fluids*, Vol. 17. pp. 103606-103616.

Truong, B., Hu, L., Buongiorno, J., & Mckrell, T. (2010). Modification of sandblasted plate heaters using nanofluids to enhance pool boiling critical heat flux. *Int. J Heat Mass Transfer*, Vol. 53, pp. 85-94.

Vafaei, S. & Wen, D. (2010). Critical Heat Flux (CHF) of Subcooled Flow Boiling of Alumina Nanofluids in a Horizontal Microchannel. *J Heat Transfer*, Vol. 132, pp. 102404-1-102404-7.

Wang, C. H. & Dhir, V. K. (1993). Effect of surface wettability on active nucleate site density during pool boiling of water on a vertical surface. *Trans. ASME J Heat Transfer*, Vol. 115, pp. 670-679.

Wasekar, V. M., & Manglik, R. M. (1999). A review of enhanced heat transfer in nucleate pool boiling of aqueous surfactant and polymeric solutions. J. *Enhanced Heat Transfer*, Vol. 6, pp. 135-150.

Watanabe, K., Yanuar and Udagawa, H. (1999). Drag reduction of Newtonian fluid in a circular pipe with a highly water-repellent wall. *J Fluid Mech.*, Vol. 381, pp. 225-238.

Wen, D. S., & Wang, B. X. (2002). Effects of surface wettability on nucleate pool boiling heat transfer for surfactant solutions. *Int. J Heat Mass Transfer*, Vol. 45. pp. 1739-1747.

Wenzel, R. N. (1936). Resistance of solid surface to wetting by water. *Ind. Eng. Chem.*, Vol. 28, pp. 988-994.

Whyman, G., Bormashenko, E. & Stein, T. (2008). The rigirious derivation of Young, Cassie–Baxter and Wenzel equations and the analysis of the contact angle hysteresis phenomenon. *Chemical Physics Letters*, Vol. 450, pp. 355–359.

Wu, H.Y. & Cheng, P. (2003). An experiment study of convective heat transfer in silicon microchannels with different surface conditions. *Int. J Heat Mass Transfer*, Vol. 46, pp. 2547-2556.

You, S. M., Bar-Cohen, A. & Simon, T. W. (1990). Boiling Incipience and Nucleate Boiling Heat Transfer of Highly Wetting Dielectric Fluids from Electronic Materials. *IEEE Transactions on Components, Hybrids, and Manufacturing Technology*, Vol. 13, No. 4, pp. 1032-1039.

Young, T. (1805). An Essay on the Cohesion of Fluids. *Phil. Trans. R. Soc. Lond.*, Vol. 95, pp. 65–87.

Yu, H., Soolaman, D. M., Rowe, A. W. & Banks, J. T. (2004). Evaporation of Water Microdroplets on Self-Assembled Monolayers: From Pinning to Shrinking. *Chem Phys Chem*, Vol. 5, pp. 1035-1038.

Zhang, W., Liu, G., Xu, J. & Yang, Y. (2009). Effect of channel surface wettability and temperature gradients on the boiling flow pattern in a single microchannel. *J Micromech. Microeng.*, Vol. 19, pp. 055012 (13pp).

Zhao, H. & Beysens, D. (1995) From Droplet Growth to Film Growth on a Heterogeneous Surface: Condensation Associated with a Wettability Gradient. *Langmuir*, Vol. 11, pp. 627-634.
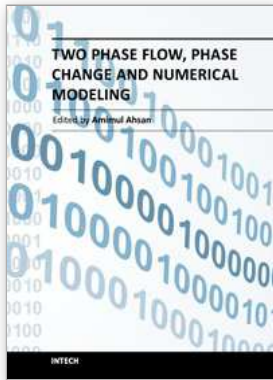
Two Phase Flow, Phase Change and Numerical Modeling

Edited by Dr. Amimul Ahsan

The heat transfer and analysis on laser beam, evaporator coils, shell-and-tube condenser, two phase flow, nanofluids, complex fluids, and on phase change are significant issues in a design of wide range of industrial processes and devices. This book includes 25 advanced and revised contributions, and it covers mainly (1) numerical modeling of heat transfer, (2) two phase flow, (3) nanofluids, and (4) phase change. The first section introduces numerical modeling of heat transfer on particles in binary gas-solid fluidization bed, solidification phenomena, thermal approaches to laser damage, and temperature and velocity distribution. The second section covers density wave instability phenomena, gas and spray-water quenching, spray cooling, wettability effect, liquid film thickness, and thermosyphon loop. The third section includes nanofluids for heat transfer, nanofluids in minichannels, potential and engineering strategies on nanofluids, and heat transfer at nanoscale. The forth section presents time-dependent melting and deformation processes of phase change material (PCM), thermal energy storage tanks using PCM, phase change in deep CO_2 injector, and thermal storage device of solar hot water system. The advanced idea and information described here will be fruitful for the readers to find a sustainable solution in an industrialized society.

How to reference

In order to correctly reference this scholarly work, feel free to copy and paste the following:

Chiwoong Choi and Moohwan Kim (2011). Wettability Effects on Heat Transfer, Two Phase Flow, Phase Change and Numerical Modeling, Dr. Amimul Ahsan (Ed.), ISBN: 978-953-307-584-6, InTech, Available from: http://www.intechopen.com/books/two-phase-flow-phase-change-and-numerical-modeling/wettability-effects-on-heat-transfer

INTECH
open science | open minds